J|A|C|S COMMUNICATIONS

Published on Web 05/27/2010

Photoinduced Metal-to-Metal Charge Transfer toward Single-Chain Magnet

Tao Liu, Yan-Juan Zhang, Shinji Kanegawa, and Osamu Sato*

Institute for Materials Chemistry and Engineering, Kyushu University, 6-1 Kasuga-koen, Fukuoka 816-8580, Japan

Received April 2, 2010; E-mail: sato@cm.kyushu-u.ac.jp

Single-chain magnets (SCMs) that exhibit slow relaxation of their magnetization are popular topics in chemistry, physics, and materials science.[1] Although various SCMs have been designed and prepared, it is a challenge to tune their properties with external stimuli such as light, heat, and pressure.[2] Photoinduced magnetization has recently become an important subject because light is a very useful and powerful tool for controlling the magnetic properties of molecular compounds.[3] Light- or heat-induced metal-to-metal charge transfers (MMCTs) must be highly effective to produce photoinduced SCMs, because the MMCT process involves concomitant spin-state and anisotropy changes at the metal centers. Herein, through the light- and heat-induced transformation between diamagnetic $Fe^{II}_{LS}(\mu\text{-CN})Co^{III}_{LS}$ (LS = low spin) units and paramagnetic $Fe^{III}_{LS}(\mu\text{-CN})Co^{II}_{HS}$ (HS = high spin) units, we show the photoswitched transformation from a paramagnetic state to an antiferromagnetic ordered SCM state and the thermally induced reverse transformation.

To obtain a photoswitchable SCM, we focused on a CN-bridged $Fe^{III}_2Co^{II}$ double zigzag chain system. SCM behaviors have been reported for such a system,[4] but no MMCT was observed because Co^{II} possesses a relatively weak ligand field through a N_4O_2 coordination sphere. To achieve an appropriate ligand field for MMCT, we attempted to increase the ligand field around Co^{II} by replacing the weakly coordinated water molecules with a long ditopic spacer possessing two potential nitrogen coordination sites, thus producing well isolated chains wherein the Co^{II} possesses a N_6 coordination sphere. Such $Fe^{III}_2Co^{II}$ compounds would potentially exhibit thermally induced and photoinduced MMCT, allowing us to observe tunable spin states and spin topology in the SCMs.

The reaction of $Li[Fe(bpy)(CN)_4]$ (bpy = 2,2′-bipyridine), $Co(ClO_4)_2\cdot 6H_2O$, and 4,4′-bipyridine in water produced block-shaped crystals of $\{[Fe(bpy)(CN)_4]_2Co(4,4'\text{-bipyridine})\}\cdot 4H_2O$ (**1**). Single crystal X-ray diffraction (XRD) analysis revealed that **1** crystallizes in a *C*2/*m* space group, with the crystal structure comprising neutral bimetallic $[Fe(bpy)(CN)_4]_2Co(4,4'\text{-bipyridine})$ layers with uncoordinated water molecules located between the layers. Within the neutral layer, the $[Fe(bpy)(CN)_4]^-$ unit acted as a bis-monodentate bridging ligand toward two Co^{II} ions through two of its four cyanide groups in the *cis* position, while each Co^{II} coordinated to four nitrogen atoms from the CN^- bridges, affording bimetallic double-zigzag chains (Figure 1a). The mean planes (Fe_2Co_2) of the square units were parallel to each other, in contrast with other reported Fe_2Co double-zigzag chains, where the mean planes (Fe_2Co_2) of the square units usually show a dihedral angle.[4] The chains were further linked by 4,4′-bipyridine ligands along the apical direction of the cobalt centers, affording a layered framework (Figure 1b). Each layer interlocked with its neighbors, affording one-dimensional channels filled with uncoordinated water molecules (Figure S1). The crystal structure consisted of one unique iron center and one unique cobalt center. Two nitrogen atoms from the bpy unit and four cyanide carbon atoms coordinated to each iron center, and each cobalt center was located in the elongated N_6 octahedral environment with four shorter equatorial Co−N distances and two longer apical Co−N distances (Figure 1a), suggesting a negative anisotropy constant *D* that is essential for SCM behavior. At 270 K, the Fe−C and Co−N bond distances were 1.911−1.952 and 2.123−2.154 Å, respectively. Valence sum bond analysis and charge compensation indicated that the cobalt centers were Co^{II}_{HS}, while the iron centers were Fe^{III}_{LS}, forming $Fe^{III}_{LS}(\mu\text{-CN})Co^{II}_{HS}$ linkages. The shortest interchain Fe···Fe and Co···Co distance was 8.849 and 10.631 Å, respectively. However, when crystals of **1** were slowly cooled, the Co−N bond distances were shortened to 1.971−2.028 Å at 173 K and 1.927−1.999 Å at 100 K, respectively. The Co−N bond distances at 173 and 100 K were significantly shorter than those expected for Co^{II}_{HS} (≈ 2.1 Å), but slightly longer than those expected for Co^{III}_{LS} (≈ 1.9 Å). These temperature dependent structural variations suggested that intramolecular charge transfer converted partial $Fe^{III}_{LS}(\mu\text{-CN})Co^{II}_{HS}$ units into $Fe^{II}_{LS}(\mu\text{-CN})Co^{III}_{LS}$ units.

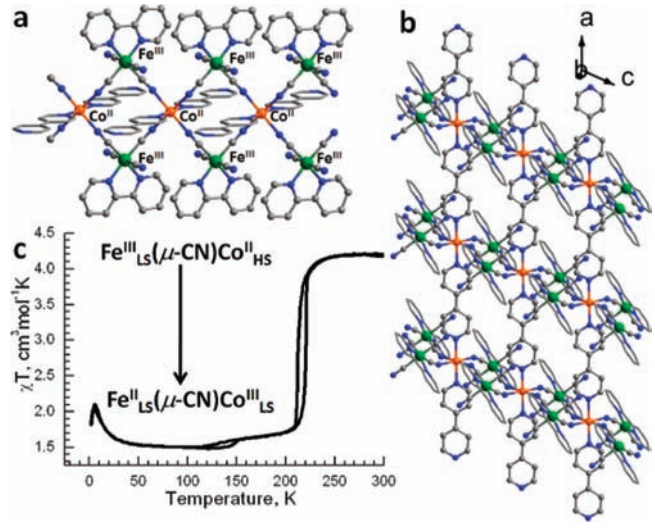

Figure 1. (a) Side view of the 1D double zigzag chain. (b) Side view of the layer formed by linking the double-zigzag chain with 4,4′-bipyridine along the *a* directions. H atoms are omitted for clarity. Atomic scheme: Fe, green; Co, orange; C, gray; N, blue. (c) Temperature dependent susceptibilities of **1** in χT vs *T*.

Additional support for this partial intramolecular electron-transfer could be found in the temperature dependent infrared (IR) spectroscopy studies of **1** (Figure S2), between 10 and 300 K. At 300 K, we observed two cyano stretching absorptions (ν_{CN}), corresponding to the free ν_{CN} absorption (2124 cm^{-1}) of $[Fe^{III}(bpy)(CN)_4]^-$ and the bridging ν_{CN} absorption (2150 cm^{-1}) of $Fe^{III}_{LS}(\mu\text{-CN})Co^{II}_{HS}$ linkages. As the temperature decreased, new stretches were observed, which were attributed to the free ν_{CN} absorption of $Fe^{II}(bpy)(CN)_4^{2-}$ (2072 cm^{-1}) and the bridging ν_{CN} absorption of $Fe^{II}_{LS}(\mu\text{-CN})Co^{II}_{HS}$ (2090 cm^{-1}), $Fe^{II}_{LS}(\mu\text{-CN})Co^{III}_{LS}$ (2109 cm^{-1}), and $Fe^{III}_{LS}(\mu\text{-CN})Co^{III}_{LS}$ (2166 cm^{-1}) linkages.[5] Such

10.1021/ja1027953

IR results confirmed that only partial Fe^{III} and Co^{II} were involved in the MMCT process. Moreover, these temperature-induced changes in the IR of **1** were completely reversible upon warming the samples, indicating the induction of the reversible MMCT.

Magnetic measurements verified the MMCT in **1**. At room temperature, the χT product was 4.20 $cm^3\ mol^{-1}K$ per Fe_2Co unit, corresponding to the presence of one Co^{II}_{HS} and two Fe^{III}_{LS} with significant orbital contributions. On cooling, the χT values remained nearly constant between 300 and 250 K (Figure 1c). However, slowly decreasing the temperature (0.5 K min^{-1}) from 250 to 200 K afforded a steep decrease in the χT products, reaching 1.70 $cm^3\ mol^{-1}$ K at 200 K. In contrast, on heating (0.5 K min^{-1}), the χT values increased and returned to the initial value with a small thermal hysteresis loop. Such a magnetic feature confirmed a reversible charge-transfer process that involved transformation between the high-temperature (HT) phase with Fe^{III}_{LS} ($S = 1/2$) and Co^{II}_{HS} ($S = 3/2$) metal ions and the low-temperature (LT) phase with diamagnetic Fe^{II}_{LS} ($S = 0$) and Co^{III}_{LS} ($S = 0$) centers. According to the χT values, ~2/3 Co^{II}_{HS} changed to Co^{III}_{LS} from the HT phase to the LT phase. Hence, the transformation could be expressed as $\{[Fe^{III}(bpy)(CN)_4]_2$-$Co^{II}$(4,4′-bipyridine)$\}\cdot 4H_2O \leftrightarrows [Fe^{II}(bpy)(CN)_4]_{2/3}[Fe^{III}(bpy)(CN)_4]_{4/3}Co^{III}_{2/3}$-$Co^{II}_{1/3}$(4,4′-bipyridine)$\}\cdot 4H_2O$. As the temperature further decreased from 200 K, another small thermal hysteresis was observed between 156 and 106 K, which may be due to structural transformation. The χT values then increased to a maximum at 6.0 K, before decreasing due to zero-field splitting and/or antiferromagnetic interactions. Further magnetic investigation revealed that the LT phase showed paramagnetic behavior as expected for discrete clusters (Figures S3, S4).

To probe the possibility of photoinduced magnetization, the IR spectra after irradiating were measured. Irradiating with a 532 nm laser light decreaseed the IR peaks due to the LT phase and produced the spectra of the HT phase (Figure S2). Hence, irradiating the LT phase induced a valence state change from the Fe^{II}_{LS}-Co^{III}_{LS} state to the Fe^{III}_{LS} -Co^{II}_{HS} state.

After irradiating, the spin topology changed from discrete clusters to one-dimensional, and SCM behavior would be expected considering the negative anisotropy constant D of Co^{II}, strong intrachain magnetic interaction transmitted via the cyanide bridge, and weak interchain magnetic interaction transmitted via 4,4′-bipyridine and hydrogen bonding. Upon light irradiation at 5 K for more than 12 h, a significant increase in χT values was observed (Figure 2a) because of the photoinduced transformation from diamagnetic $Fe^{II}_{LS}(\mu$-$CN)Co^{III}_{LS}$ to metastable paramagnetic $Fe^{III}_{LS}(\mu$-$CN)Co^{II}_{HS}$ units. On heating, the χT values first increased steeply to a sharp maximum of 35.7 $cm^3\ mol^{-1}$ K at 4.4 K, then decreased gradually, and, at ~100 K, overlapped with the plots of before photoirradiation. The sigmoidal shape of the field dependent magnetizations at 1.8 K (Figure S5) featured the field-induced transition from an antiferromagnetic state to a ferromagnetic state without obvious hysteresis, indicating that the interchain interactions were antiferromagnetic. Coulon *et al*. demonstrated that the antiferromagnetic interaction between SCMs stabilized a 3D antiferromagnetic ordering without preventing the slow relaxation of the magnetization induced by the SCM components of the material.[6] To investigate the dynamics of the magnetization, the alternative current (ac) magnetic susceptibility was studied as a function of both temperature and frequency. Variable-temperature ac susceptibility measurements revealed a strong frequency dependence of both in-phase (χ') and out-of-phase components (χ''), as observed in other SCMs.[7] From these data, relaxation times have been estimated and fit to Arrhenius laws (Figure S6), providing a pre-exponential factor of $\tau_0 = 1.4 \times 10^{-9}$ s and a relaxation energy barrier of $\Delta_\tau/k_B = 29$ K.

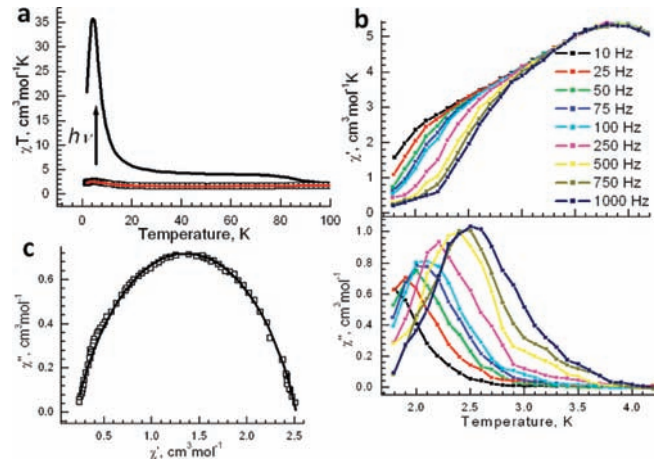

Figure 2. (a) Temperature dependent susceptibilities of **1** before irradiating (red line), after irradiating (black line), and after thermally treating up to 150 K (□). (b) Temperature dependence of the real and imaginary parts of the ac susceptibility for **1** after irradiating in zero dc-field at varying ac frequency and with a 3 Oe ac field. (c) Cole−Cole diagram (□) for **1** after irradiating at 1.85 K. The solid line represents the best fit of the experimental results with a generalized Debye model.

The in-phase ac susceptibility showed a frequency independent peak at 3.8 K, which might be due to the weak interchain antiferromagnetic interactions, as suggested by the fact that the maximum of χ'' decreased with decreasing frequency.[7] A semicircular Cole−Cole diagram (χ'' versus χ', Figure 2c) was constructed from the variable-frequency data collected at 1.85 K and was fit to a generalized Debye model,[8] giving an α value of 0.34. This analysis demonstrated that the state of **1** after irradiation was an antiferromagnetic ordered phase of SCMs.

In summary, through the exploitation of the light-induced transformation from diamagnetic $Fe^{II}_{LS}(\mu$-$CN)Co^{III}_{LS}$ to paramagnetic $Fe^{III}_{LS}(\mu$-$CN)Co^{II}_{HS}$ units, we have shown that an antiferromagnetic ordered SCM can be photoswitched from paramagnetic discrete clusters. The reverse transformation can be thermally switched, providing an effective way to control the spin topology of the SCM via light- or a thermally induced metal-to-metal charge transfer.

Supporting Information Available: X-ray crystallographic file in CIF format for **1**, a PDF file containing further information about the experiments, Tables S1−S4, and Figures S1−S6. This material is available free of charge via the Internet at http://pubs.acs.org.

References

(1) (a) Caneschi, A.; Gatteschi, D.; Lalioti, N.; Sangregoril, C.; Sessoli, R.; Venturi, G.; Vindigni, A.; Rettori, A.; Pini, M. G.; Novak, M. A. *Angew. Chem., Int. Ed.* **2001**, *40*, 1760. (b) Miyasaka, H.; Julve, M.; Yamashita, M.; Clérac, R. *Inorg. Chem.* **2009**, *48*, 3420.

(2) Morimoto, M.; Miyasaka, H.; Yamashita, M.; Irie, M. *J. Am. Chem. Soc.* **2009**, *131*, 9823.

(3) (a) Sato, O.; Tao, J.; Zhang, Y.-Z. *Angew. Chem., Int. Ed.* **2007**, *46*, 2152. (b) Ohkoshi, S.; Hamada, Y.; Matsuda, T.; Tsunobuchi, Y.; Tokoro, H. *Chem. Mater.* **2008**, *20*, 3048. (c) Li, D.-F.; Clérac, R.; Roubeau, O.; Harté, E.; Mathonière, C.; Bris, R. L.; Holmes, S. M. *J. Am. Chem. Soc.* **2008**, *130*, 252.

(4) Lescouëzec, R.; Vaissermann, J.; Ruiz-Pérez, C.; Lloret, F.; Carrasco, R.; Julve, M.; Verdaguer, M.; Dromzée, Y.; Gatteschi, D.; Wernsdorfer, W. *Angew. Chem., Int. Ed.* **2003**, *42*, 1430.

(5) Escax, V.; Bleuzen, A.; Moulin, C. C. d.; Villain, F.; Goujon, A.; Varret, F.; Verdagure, M. *J. Am. Chem. Soc.* **2001**, *123*, 12536.

(6) Coulon, C.; Clérac, R.; Wernsdorfer, W.; Colin, T.; Miyasaka, H. *Phys. Rev. Lett.* **2009**, *102*, 167204–1.

(7) (a) Harris, H. D.; Bennett, M. V.; Clérac, R.; Long, J. R. *J. Am. Chem. Soc.* **2010**, *132*, 3980. (b) Miyasaka, H.; Takayama, K.; Saitoh, A.; Furukawa, S.; Yamashita, M.; Clérac, R. *Chem.—Eur. J.* **2010**, *16*, 3656.

(8) Aubin, S. M. J.; Sun, Z.; Pardi, L.; Krzystek, J.; Folting, K.; Brunel, L.-C.; Rheingold, A. L.; Christou, G.; Hendrickson, D. N. *Inorg. Chem.* **1999**, *38*, 5329.

JA1027953